Large-scale fluid/fluid phase separation of proteins and lipids in giant plasma membrane vesicles

Tobias Baumgart*, Adam T. Hammond†, Prabuddha Sengupta†, Samuel T. Hess‡, David A. Holowka†, Barbara A. Baird†, and Watt W. Webb*§

*School of Applied and Engineering Physics and †Department of Chemistry and Chemical Biology, Cornell University, Ithaca, NY 14853; and ‡Department of Physics and Astronomy, University of Maine, Orono, ME 04469

Contributed by Watt W. Webb, December 26, 2006 (sent for review September 21, 2006)

The membrane raft hypothesis postulates the existence of lipid bilayer membrane heterogeneities, or domains, supposed to be important for cellular function, including lateral sorting, signaling, and trafficking. Characterization of membrane lipid heterogeneities in live cells has been challenging in part because inhomogeneity has not usually been definable by optical microscopy. Model membrane systems, including giant unilamellar vesicles, allow optical fluorescence discrimination of coexisting lipid phase types, but thus far have focused on coexisting optically resolvable fluid phases in simple lipid mixtures. Here we demonstrate that giant plasma membrane vesicles (GPMVs) or blebs formed from the plasma membranes of cultured mammalian cells can also segregate into micrometer-scale fluid phase domains. Phase segregation temperatures are widely spread, with the vast majority of GPMVs found to form optically resolvable domains only at temperatures below ≈25°C. At 37°C, these GPMV membranes are almost exclusively optically homogenous. At room temperature, we find diagnostic lipid phase fluorophore partitioning preferences in GPMVs analogous to the partitioning behavior now established in model membrane systems with liquid-ordered and liquid-disordered fluid phase coexistence. We image these GPMVs for direct visual characterization of protein partitioning between coexisting liquid-ordered-like and liquid-disordered-like membrane phases in the absence of detergent perturbation. For example, we find that the transmembrane IgE receptor FcεRI preferentially segregates into liquid-disordered-like phases, and we report the partitioning of additional well known membrane associated proteins. Thus, GPMVs now provide an effective approach to characterize biological membrane heterogeneities.

liquid-disordered | liquid-ordered | membrane domains | membrane heterogeneity | rafts

The membrane raft hypothesis proposes that membrane lipid domains enriched in cholesterol and sphingolipids form dynamic sorting and signaling platforms for membrane proteins (1). Consensus data on the size, lifetime, and even existence of lipid rafts in intact plasma membranes, however, have been elusive (2, 3). Controversy arises due to current experimental ambiguity and to operational definitions of membrane lipid heterogeneity.

One common definition has relied on biochemical assessment of membrane heterogeneity involving membrane lysis using certain nonionic detergents, such as Triton X-100 at 4°C (4). A second, operational definition for lipid rafts has been cellular processes that are perturbed by either cholesterol or sphingomyelin depletion. Problems of these approaches have been extensively discussed (2, 3).

The reports that membranes composed of lipids that are resistant to detergent solubilization are apparently in a liquid-ordered (L_o) state (5–7) have been the basis for proposing that lipid rafts in plasma membranes represent the L_o phase of coexisting L_o and liquid-disordered (L_d) fluid/fluid phases (2, 8). Biological membrane heterogeneity, however, cannot be reduced to partitioning between coexisting lipid domains, because reciprocal protein–lipid, as well as protein–protein interactions necessarily modulate the thermodynamics of lipid heterogeneity (2, 9, 10), emphasizing the need for examining membranes with significant protein content, as suggested by protein segregation measurements on living cells (11).

Several studies have suggested the existence of membrane heterogeneities with size scales below optical resolution (≈300 nanometers), but estimates of lipid raft sizes in the literature range from several micrometers, as in cholesterol-depleted cells (12), to just a few molecules (13). Fluid/fluid phase separation in biological cell membranes has thus far not been unequivocally demonstrated in live cells, perhaps because coupling of the plasma membrane to the underlying cytoskeleton may prevent fluid phase segregation into distinctive domains, as can be observed in lipid-only model membranes with appropriate compositions. Differences from model membranes could arise from the pinning of plasma membrane domains by cytoskeleton-attached, membrane-associated proteins or from complex membrane rugosities induced by protein–protein interactions. Furthermore, the enormous complexity of cellular plasma membrane protein and lipid compositions might preclude the simple fluid/fluid phase separations observed in ternary lipid mixtures (14).

To investigate fluid/fluid phase coexistence in systems with realistic biological membrane compositions, we here use giant plasma membrane vesicles (GPMVs) that are derived from biological cells, RBL mast cells, and fibroblasts by chemically induced plasma membrane vesiculation or "blebbing" (15–17). These GPMVs show simple, low-curvature geometries of giant unilamellar vesicles and appear free of cytoskeletal constraints. By using fluorophores providing recently characterized membrane fluid phase partitioning behavior (T.B., G. Hunt, E. R. Farkas, W.W.W., and G. W. Feigenson, unpublished data) for lipid phase characterization here, we find that these GPMVs can segregate into multi-micrometer-scale coexisting fluid phases, thereby enabling extension of early cell blebbing studies in our laboratories in the 1980s (15, 18–20). These results are noted and used throughout this paper.

Results

In initial experiments to study phase separation in plasma membrane-derived, micrometer-scale vesicles, mammalian cells

Author contributions: T.B., S.T.H., and W.W.W. initiated research; T.B. P.S., S.T.H., and A.T.H. performed research; T.B., A.T.H., P.S., S.T.H., D.A.H., and B.A.B. analyzed data; and T.B., D.A.H., B.A.B., and W.W.W. wrote the paper.

The authors declare no conflict of interest.

Abbreviations: CM, laser scanning confocal microscopy; CTB, cholera toxin subunit B; GPMV, giant plasma membrane vesicle; GUV, giant unilamellar vesicle; L_d, liquid-disordered; L_o, liquid-ordered; Nap, naphthopyrene; R-DOPE, rhodamine B sulfonyl dioleoyl phosphatidyl ethanolamine.

§To whom correspondence should be addressed at: Cornell University, 212 Clark Hall, Ithaca, NY 14853. E-mail: www2@cornell.edu.

This article contains supporting information online at www.pnas.org/cgi/content/full/0611357104/DC1.

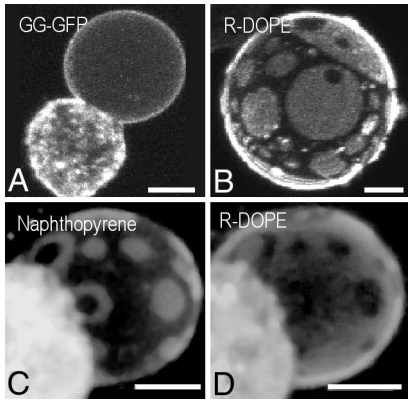

Fig. 1. Cell-attached GPMVs can laterally segregate into coexisting fluid phases. (*A*, *C*, and *D*) RBL cells treated with 4% (vol/vol) ethanol. Cells containing fluorescent membrane probes show formation of large GMPVs attached to the cell bodies by superposition of CM or two-photon microscopy image *z*-stacks. (*A*) Cell expressing geranylgeranyl-EGFP (GG-GFP) with attached GPMV measured by CM-imaged stack at ≈23°C. Note the absence of internal membranes within the GPMV and significant partitioning of GG-GFP into the GPMV compared with the cell body structures. (*B*) CM images of an NIH 3T3 GPMV incubated at room temperature with 1% (vol/vol) DMSO and R-DOPE, showing large-scale fluid/fluid phase coexistence similar to the RBL cells. (*C* and *D*) Two-photon microscopy images of a cell-attached GPMV colabeled with the membrane markers Nap (*C*) and R-DOPE (*D*), imaged at 5°C. Note their contrasting wavelength-selected labeling of the separated phases. Cell bodies show large fluorescence (attenuated here) due to internalized membrane probes. (Scale bars, 5 μm.)

were treated with combinations of polar organic solvents to induce GPMV formation and selected membrane dyes to label lipid phases. Fig. 1 illustrates typical fluorescence-labeled cell-attached GPMVs imaged by stacks of laser scanning confocal microscopy (CM) or two-photon microscopy sections. The GPMV in Fig. 1*A* was induced by addition of 4% (vol/vol) ethanol to suspended RBL cells, and GPMV in Fig. 1*B* was induced by addition of DMSO (1% vol/vol) to adherent fibroblasts. Under these conditions, substantial membrane dye is rapidly internalized, delivering fluorescence to the cell body, as illustrated in Fig. 1 *A*, *C*, and *D*. These GPMVs, having dimensions comparable to cell sizes, occur in low fractions (<5%) of treated cells and are possibly induced by transient, local high solvent concentration during solvent injections into the surrounding buffer. The cell-attached GPMV on an RBL cell in Fig. 1*A* was prelabeled by the plasma membrane inner-leaflet-targeted protein, geranylgeranyl-EGFP (21), and it shows a homogenous membrane bilayer at optical resolution when imaged at room temperature. Fig. 1*B* shows a lipid phase-separated GPMV from NIH 3T3 fibroblasts labeled with lissamine rhodamine B sulfonyl dioleoyl phosphatidyl ethanolamine (R-DOPE) to demonstrate that plasma membrane fluid/fluid phase separation at room temperature is not a unique property of GPMVs obtained from RBL mast cells.

At temperatures of 4–10°C, cell-attached GPMV membranes often separate into two distinct phases, as shown by the contrasting fluorescence patterns of naphthopyrene (Nap) in Fig. 1*C* and R-DOPE in Fig. 1*D*. That these coexisting domains are in fluid phase states at 4°C is indicated by frequent coalescence activity and circular morphology. The fluid phase separations shown in Fig. 1 *C* and *D*, as well as all other phase-separated GPMVs examined here, show only two different fluorescence intensities, suggesting that the lipid domains are coupled across the bilayer, as previously observed for inner- and outer-leaflet-labeled domain registration in phase-separated model membrane giant unilamellar vesicles (GUVs) (22).

Nap preferentially labels the L_o phase in model membranes containing ternary lipid mixtures of brain sphingomyelin, dioleoyl phosphatidylcholine, and cholesterol, whereas R-DOPE strongly prefers L_d membranes coexisting with L_o domains over wide ranges of differing lipid compositions (T.B., G. Hunt, E. R. Farkas, W.W.W., and G. W. Feigenson, unpublished data). Thus, GPMVs from RBL cells appear to phase-separate into coexisting fluid membrane phases with L_o-like and L_d-like phase states. Because membrane phase behavior is likely to be modified in the presence of organic solvents, we also developed alternative protocols for GPMV formation and membrane staining.

Membrane blebbing induced by chemical methods that modify amino and sulfhydryl groups (15, 17, 23) allows isolating large numbers of GPMVs from adhering cells for characterization (15, 24). GPMVs isolated after treatment of RBL mast cells with 25 mM formaldehyde, together with 2 mM DTT, or by treatment with 2 mM *N*-ethylmaleimide for 1 h at 37°C phase separate in a temperature-dependent manner. Representative low-magnification views of cell-free GPMVs isolated after formaldehyde/DTT treatment and labeled with the L_d phase-preferring fluorescent phospholipid R-DOPE were imaged at three different temperatures [supporting information (SI) Fig. 4]. At 5°C, essentially all vesicles phase separate (SI Fig. 4*A*), but at room temperature only ≈10–25% of all vesicles show large-scale fluid/fluid phase coexistence (SI Fig. 4*B*). At 37°C, fluid phase coexistence is rare: <1% of all imaged GPMVs show optically resolvable domains. One of these exceptional cases is depicted in SI Fig. 4*C Inset*. The large variation in phase separation observed in different vesicles, especially at intermediate temperatures, may indicate compositional variations among GPMVs in these preparations.

Fig. 2 compares the fluid-phase partitioning behavior of several lipid analogues (Nap, R-DOPE, and DiI C16:0) and lipid-binding proteins [cholera toxin subunit B (CTB) and annexin V] in cell-free GPMVs imaged at room temperature (Fig. 2 *A–C*) and at 12°C (Fig. 2*D*). Nap and R-DOPE show contrasting partitioning in coexisting fluid phases, both at room temperature as shown in Fig. 2*A* and at 5°C (Fig. 1 *C* and *D*). Fig. 2*B* shows that CTB bound to the ganglioside GM_1 partitions into membrane regions complementary to those labeled with L_d-preferring R-DOPE. CTB is frequently used as a marker for cellular lipid rafts and caveolae based on sucrose gradient fractionation experiments (25), and GUV model membrane studies have shown that fluorescent CTB bound to GM_1 preferentially labels L_o phases that are coexisting with L_d phases (26, 27). Partitioning of CTB bound to GM_1, in contrast to DiI C16:0, indicates that DiI preferentially partitions into the L_d-like phase (Fig. 2*C*). Although DiI C16:0 is deemed a marker for lipid rafts on cells (12, 28, 29), it has been observed to partition preferentially into L_d phases in selected ternary mixtures of brain sphingomyelin/dioleoyl phosphatidylcholine/cholesterol and in mixtures of distearoyl phosphatidylcholine/dioleoyl phosphatidylcholine/cholesterol (data not shown).

We compared the partitioning of CTB bound to GM_1 with fluorescent annexin V, which binds phosphatidylserine (PS) in a calcium-dependent manner (30). Annexin V is an indicator of transbilayer flipping of the negatively charged PS that is a hallmark of cellular apoptosis (31). In phase-separated GPMVs, annexin V labeling is in contrast to L_o-like domains that are preferentially labeled with fluorescent CTB (Fig. 2*D*). This indicates that PS, and possibly other negatively charged phospholipids, partition preferentially into more disordered regions of these GPMVs. Noting that phase separation in vesicles labeled with fluorescent CTB and annexin V derivatives is similar to lipid-bound fluorophores (R-DOPE, DiIC16:0, and Nap) excludes the possibility that the fluid phase segregation we detect is due to membrane insertion of fluorescent lipids or to photodecomposition products of membrane-embedded fluorophores.

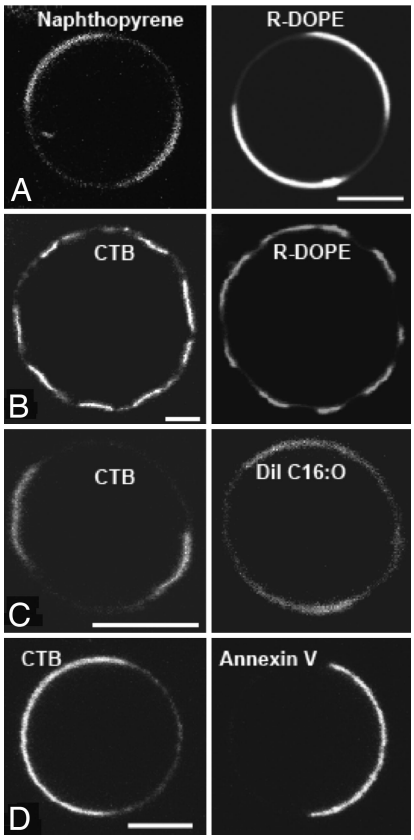

Fig. 2. Plasma membrane lipids and lipid fluorophores in GPMVs demonstrating characteristic phase preferences resembling the L_o/L_d partitioning behavior in model membranes. GPMVs, all prepared by formaldehyde/DTT treatment of RBL cells, were colabeled by Nap, R-DOPE, or DiIC16 and by A488-CTB bound to GM_1 or A568-annexin V bound to phosphatidylserine. Images are equatorial CM sections obtained at ≈23°C. (*A*) GPMVs colabeled with Nap and R-DOPE show contrasting partitioning. (*B*) GPMVs colabeled with CTB and R-DOPE show contrasting partitioning. (*C*) GPMVs colabeled with CTB and DiI C16:0 show contrasting partitioning. (*D*) CTB/annexin V-colabeled GPMV shows contrasting partitioning, indicating that annexin V labels an L_d-like phase.

Photoinduced lipid oxidation, which can interfere with membrane phase behavior (32), was minimized by the antioxidant DTT.

As seen by CM, soluble fluorescently labeled proteins, such as CTB and annexin V, are mostly excluded from the interior of GPMVs, suggesting that their membranes are sufficiently sealed to prevent internalization of protein-sized solutes. However, some GPMVs are slightly leaky to these proteins, as judged by the occasional observation of slow internal labeling of GPMVs (data not shown). Nevertheless, determining whether fluorescent annexin V on GPMVs is labeling phosphatidylserine flipped to the outer leaflet or on the inner leaflet of these GPMVs is uncertain. Earlier experiments on formaldehyde induced plasma membrane vesicles of neuroblastoma cells indicated partial retention of lipid asymmetry for as long as 3 days after blebbing at 37°C for 1.5–2 h and subsequent storage at 4°C (33), suggesting that GPMVs may retain significant leaflet asymmetry during our imaging, but it remains for future studies to determine the extent of lipid asymmetry preservation in GPMVs.

An advantage of GPMVs is that membrane protein partitioning can be reliably studied by optical microscopy in vesicles with clearly identified fluid/fluid phase coexistence. Fig. 3 demonstrates selective partitioning of lipid-anchored proteins from outer and inner leaflets of cellular plasma membranes, as well as partitioning of a transmembrane protein complex. Glycosylphosphatidylinositol-anchored proteins, including Thy-1, are common markers for outer leaflets of lipid rafts, based on detergent fractionation, (34, 35), intact cell membrane (36, 37), and model membrane studies (38). Fig. 3*A* shows Thy-1 labeled with Cy3-conjugated Ox7 mAb partitioning preferentially into the L_o-like phase in GPMVs with fluid/fluid phase coexistence. In contrast, several lipid-anchored proteins that localize to the inner leaflet of the plasma membrane were found to partition preferentially into the L_d-like phase.

Fig. 3*B* shows that Lyn-GFP, which reconstitutes FcεRI-mediated signaling (39, 40), partitions preferentially into the L_d phase of GPMVs. However, several sucrose gradient analysis studies had suggested that Lyn itself preferentially associates with "lipid rafts" under a variety of cell lysis conditions (39, 41, 42). Similarly, the GFP chimera PM-GFP, which is anchored to the plasma membrane inner leaflet by myristate and palmitate acyl chains attached to the first 20 amino acid residues of Lyn (21), preferentially partitions into the L_d-like phase in GPMVs (Fig. 3*C*), and a geranylgeranyl-anchored chimera of GFP (21) similarly partitions into L_d-like phases (Fig. 3*D*). Sucrose gradient fractionation of detergent-lysed cells suggests that the GFP module enhances L_d partitioning (39). However, the strong L_d partitioning observed with these inner-leaflet lipid-anchored proteins in GPMVs represents a significant quantitative difference from detergent fractionation predictions.

We find that A488-labeled IgE bound to FcεRI strongly partitions into the L_d-like phase of GPMVs, as shown in Fig. 3*E*. These results are consistent with those obtained from sucrose gradient analysis of TX-100-lysed RBL cells over a large range of detergent concentrations (41, 43, 44). Cross-linking of this IgE-receptor complex has been shown to substantially increase its partitioning into detergent-resistant lipid rafts (41), and it will be interesting to investigate the effects of FcεRI cross-linking on its phase partitioning in GPMVs.

Fig. 3*F* shows that the FITC-conjugated lectin, Con A, which binds to a large number of α-methyl mannoside-containing glycoproteins and glycolipids, preferentially partitions into the L_d-like phase as well, as evidenced by colabeling with R-DOPE. Comparison of the fluorescence intensity of FITC-Con A labeling of two GPMVs attached to a cell in Fig. 3*G* shows that the glycoproteins and glycolipids that segregate into the emerging GPMVs represent a substantial fraction of the Con A binding sites on the cell surface. However, quantitative estimation of bleb protein content versus cellular membrane protein content is uncertain because of the highly folded nature of the cellular membrane, compared with the smooth bleb membranes.

GUV model membranes enable examination of mechanical aspects of membranes with fluid/fluid phase coexistence, including curvature coupling to membrane phase patterns and line tension at phase boundaries (14, 45–47), as well as experimental tests of mechanical membrane theories (14, 48). GUVs with L_o/L_d phase coexistence and relatively monodisperse domain sizes show hexagonal arrays of phase domains in superstructures that are reminiscent of modulated phase separation patterns observed in many other physical systems (49). SI Fig. 5*A* illustrates the hexagonally modulated phase patterns that also are occasionally observed in GPMVs. Modulated phase patterns can be stabilized by competing short-range attractive and long-range repulsive forces, and model membrane systems have indicated compositional variations arising from short-range attractions that couple to membrane curvature modulations, possibly leading to long-range repulsion (14, 49). These modulated patterns are likely to be kinetically trapped nonequilibrium structures subject to domain coalescence and possibly other coarsening mechanisms (50) due to line tension at phase boundaries typically leading to complete phase separation after long observation times.

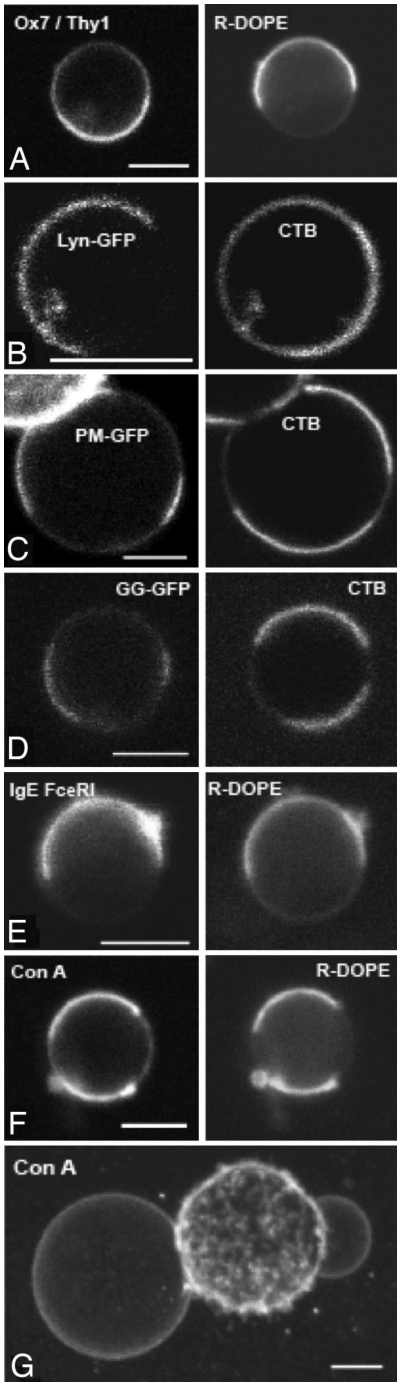

Fig. 3. GPMVs reveal membrane protein phase preferences in detergent-free GPMVs. Fluorescence images of equatorial confocal sections through GPMVs comparing the fluid phase partitioning of membrane-associated proteins (left column) to the lipid probes R-DOPE and CTB bound to GM_1 (right column). All GPMVs were prepared by formaldehyde/DTT treatment of RBL cells and imaged at ≈23°C. (*A*) GPI-anchored protein Thy-1 labeled with A488-anti-Thy1 mAb is preferentially in L_o phase, showing fluorescence in regions contrasting to R-DOPE partitioning in the L_d-like phase. (*B*) Lyn-GFP partitions preferentially into the L_d-like phase, in contrast with the CTB-labeled L_o-like phase. (*C*) PM-GFP partitions strongly into the L_d-like phase, in contrast to the CTB-enriched phase, in a cell-attached GPMV. (*D*) GG-GFP partitions preferentially into the L_d-like phase, complementary to CTB. (*E*) FcεRI labeled with A488-IgE partitions into the L_d-like phase colabeled with R-DOPE. (*F*) FITC-Con A labels glycoproteins and glycolipids that preferentially cosegregate with the L_d phase marker R-DOPE. (*G*) A significant fraction of Con A receptors populate GPMVs, compared with those in the attached cell. (Scale bar, 5 μm.)

Although domains of our phase-separated GPMVs show small curvature gradients, i.e., the membrane geometries approach circular domains on a smooth sphere, a notable exception is GPMVs with small domains that are labeled with CTB, as seen in Fig. 2*B* and SI Fig. 5*B*. Upon cholera toxin binding, preexisting L_o-like domains develop significant inward curvature. Interestingly, internalization of CTB bound to GM_1 occurs in cells in a cholesterol-dependent fashion (51), and it is possible that CTB promotes internalization by inducing a spontaneous inward curvature that facilitates budding and fission. Similar inward curvature is occasionally observed for CTB-labeled L_o domains in GUV model membranes (A.T.H., unpublished data).

Occasionally, phase-separated GPMVs show domain shapes fluctuating via in-plane domain boundary undulations. SI Fig. 5*C* shows sequential images of a vesicle at 23°C with domain undulations. These two-dimensional undulations also are observed in GUV model membranes with fluid/fluid phase coexistence near mixing/demixing transition temperatures, where line tension can become relatively small (14, 45). These undulations further highlight the presence of fluid/fluid phase coexistence in GPMVs. Fluid phase coexistence also is supported by fast recovery of spot photobleaching of all labeled lipids and membrane proteins examined here (data not shown).

Discussion

Plasma membrane vesicles, commonly called blebs, are naturally formed in a variety of physiological processes that include blebbing in locomoting cells, in cells undergoing mitosis, and in apoptotic cells. Bleb formation can be artificially induced by a variety of methods (52), including our addition of solvents or sulfhydryl group-blocking reagents. Depending on the method, different types of blebs can be obtained (52, 53). Ours were formed through cell swelling and blebbing, as in oncosis (53). These blebs have been shown to be free of cellular organelles, with lipid compositions representative of the plasma membrane, with phospholipid/cholesterol ratios of ≈2:1 (6, 16, 24). Our GPMVs from RBL cells contain constitutively active tyrosine kinase Lyn (N. Smith, D.A.H., and B.A.B., unpublished data).

A possible question is the cellular source of GPMV membranes, considering the apparent increased plasma membrane area during blebbing (see Figs. 1 and 3*G*). Membrane capacitance measurements via patch-clamping of mast cells have revealed that osmotic inflation of cells by approximately 4 times the resting volume did not change membrane conductance and only caused small reversible changes of total cell membrane capacitance (54). These results combined with the finding of exocytosis inhibition by inflation (54) suggest that GPMV membranes are likely to accrue from excess membrane area stored in membrane microvilli and various protrusions including coated pits, lamellipodia, and ruffles, but more direct comparisons are needed.

The overall protein content of GPMVs must influence membrane phase behavior. GPMVs from RBL cells have been reported to contain ≈20–25% of the cellular IgE-receptor complexes (15), roughly comparable with the apparent fraction of cellular plasma membrane extruded as GPMV. This conclusion is supported by abundant Con A labeling via their glycosylated protein binding sites retained in cell-attached GPMVs (Fig. 3*G*) and by recent ESR measurements that provided evidence for similar phase coexistence behavior in GPMV and in living cell plasma membranes (55). Earlier IgE-receptor diffusion measurements have indicated significant mobility increase due to observed reductions of molecular crowding relative to cell membranes on hypertonically swollen cells and chemically induced membrane blebs (56, 57). Extensive experiments will be required to establish the important relations between membrane phases and protein contents. We find that the F-actin probe Alexa Fluor 488 phalloidin does

penetrate the membranes and uniformly stains the volume of the GPMV plus the actin cytoskeleton in the residual cell body (data not shown), confirming the absence of a cortical actin assembly on GPMVs, as shown previously by electron microscopy (23) and flourescence microscopy (20). This uncoupling from the cortex is likely to be critical for the observed membrane phase separations. Polyphosphoinositide lipids (24, 58) and cytoskeletally immobilized proteins may be excluded from GPMVs (59, 60), a future question that needs to be addressed.

Important results of this study are the defined mixing/demixing transition temperatures in the protein-containing membranes of individual GPMVs. The significant temperature dependence of plasma membrane phase behavior also has been demonstrated recently by photobleaching recovery measurements (61). We find that individual vesicles show large variations in transition temperatures, with the vast majority of vesicles undergoing phase separations only at temperatures between ≈10°C and 25°C. These low-temperature phase separations are defined by the coexistence of two fluid membrane phases with sharp phase boundaries at optical resolution. Two distinct fluid phases do form despite the complex GPMV membrane composition, relative to simple ternary lipid mixtures of model membranes with composition-dependent fluid-phase-coexistence temperatures (38, 45, 47). Coexisting fluid membrane phases in GPMVs show fluorescence probe partitioning behavior similar to model membranes with L_o/L_d phase coexistence.

Demixing phase separations, particularly in binary or ternary systems, can be considered in regular solution theory, where an enthalpic term due to preferential molecular interactions balances against the entropic contribution proportional to temperature to determine the free energy change of mixing. Highly preferential interactions lead to lower demixing temperatures. Local concentration fluctuations associated with nonideal mixing (62) may diverge on approaching critical (consolute) points of multicomponent phase diagrams (63). Our finding of L_o/L_d-like phase separation only below physiological temperatures suggests correlated concentration fluctuations above the demixing temperatures that may lead to local composition fluctuations amenable to protein interactions. Correlated concentration fluctuations in native, macroscopically homogenous plasma membranes could yield an increased encounter probability of signaling molecules with similar membrane phase preference and, likewise, decreased encounter probabilities of signaling components with differing phase preferences. Our experiments do not yet include lifetimes or length scales of such composition fluctuations.

The large-scale development of membrane phase domains is driven by the interphase energy of the phase boundaries. Whereas this line tension at fluid phase boundaries can be substantial in lipid model membrane systems (14), line tension magnitudes could differ significantly and be much smaller in more complex membrane compositions, possibly favoring small-scale cell membrane heterogeneities (64), because line tensions are generally reduced significantly by solute segregation to the interphase boundaries.

In summary, we find that GPMVs from RBL mast cells undergo fluid phase segregation that permits the characterization of lipid and protein partitioning in complex biological membranes. These GPMVs, which contain integral and peripheral membrane proteins and hundreds of different lipids, segregate into L_o/L_d-like fluid membrane phases at low temperatures, indicating nonideal, nonrandom lateral distributions of membrane components and permitting determination of membrane phase preferences of labeled lipids and of membrane proteins. The high-affinity IgE receptor partitions into L_d-like phases, whereas a glycosylphosphatidylinositol-anchored protein and CTB bound to GM_1 segregate into L_o-like phases. Several acyl-chain-anchored, GFP-labeled proteins, including palmitoyl/myristoyl-anchored Lyn, partition preferentially to L_d-like (i.e., "non-raft") phases in GMPVs, in contrast to their reported association with detergent-resistant membrane particles, that have been hypothesized to represent "rafts." These inner-leaflet acyl-chain-anchored proteins may be affected by changes in lipid asymmetry during the formation of GPMVs.

Our method avoids membrane disruption by detergent treatment or depletion of membranes of cholesterol or sphingomyelin. The approach is suitable for examining the distribution of lipids and proteins between membrane domains and therefore allows testing predictions from the raft hypothesis in laterally intact cellular bilayer membranes. Our results present clear evidence that these complex biological cell plasma membranes can phase segregate into coexisting fluid phases but primarily at temperatures below ≈25°C. The strong temperature dependence of this segregation is consistent with expectations from model membrane studies and implies that, at temperatures above the demixing transition temperature, diffusing membrane heterogeneities may persist. Further investigation will be necessary to clarify the differences between GPMV and cellular plasma membranes in temperature-dependent phase behavior. Future studies can use GPMVs to examine the dependence of membrane protein phase partitioning on biochemical activities, including the regulation of membrane-associated kinases and phosphatases in cell signaling.

BIOPHYSICS

Materials and Methods

For lipid probes, antibodies, GFP constructs, cell culture and transfection, and imaging methods, see *SI Materials and Methods*.

GPMV Formation. GPMVs were formed by three different methods aimed to produce either cell-attached or free GPMVs of RBL cell plasma membranes.

Cell-attached GPMVs. Cell-attached GPMVs were prepared by addition of 1–5% (vol/vol) ethanol, acetone, or DMSO to RBL cells suspended at 10^6 cells per milliliter in PBS for 15 min at room temperature (23°C) or by addition of solvents to adherent NIH 3T3 cells in four-well plates. Solvents used to induce membrane vesiculation typically contained R-DOPE or DiIC16:0 at 200 μg/ml or Nap at 50 μg/ml.

Cell-Free GPMVs. Cell-free GPMVs were prepared by either of the two following methods. The primary protocol for GPMV formation used a procedure modified from Scott (16, 17) and described in ref. 15. Briefly, cells were grown to confluency in a 25-cm^2 tissue culture flask, then cells were washed twice with GPMV buffer (2 mM $CaCl_2$/10 mM Hepes/0.15 M NaCl, pH 7.4), and ≈1.5 ml of freshly prepared GPMV reagent was added, consisting of 25 mM formaldehyde and 2 mM DTT in GPMV buffer. The flasks were then incubated for 1 h at 37°C while slowly shaking (60–80 cycles per minute). After incubation, GPMVs that had detached from the cells were gently decanted into a conical tube. Previously published protocols (15) further purified the vesicles by centrifugation and dialysis, but we found that these procedures caused fragmentation of large GPMVs, making microscopic analysis difficult. For the present experiments, we allowed GPMVs to settle on ice for 10- 45 min and collected them by removing ≈20% of the total volume from the bottom of the tube. By using this method, a single confluent 25-cm^2 flask yields sufficient GPMVs to create several dozen microscopy samples.

In an alternative protocol, formaldehyde and DTT were replaced by 2 mM *N*-ethylmaleimide, a reagent previously shown to cause GPMV formation (17). All other steps are identical. The yield of GPMV is lower, and more cells detach under these conditions. Therefore, this protocol was used primarily to verify that the small amount of formaldehyde and DTT present in the primary method did not affect the results obtained.

This work was supported by Science and Technology Centers Program Agreement ECS-9876771 from the Nanobiotechnology Center of the National Science Foundation and by National Institute of Allergy and Infectious Diseases Grant R01 AI18603 and National Institute of Biomedical Imaging and Biotechnology Grant P41 EB001976.

1. Simons K, Ikonen E (1997) *Nature* 387:569–572.
2. Edidin M (2003) *Ann Rev Biophys Biomol Struct* 32:257–283.
3. Munro S (2003) *Cell* 115:377–388.
4. Brown D, Rose J (1992) *Cell* 68:533–544.
5. Schroeder R, London E, Brown D (1994) *Proc Natl Acad Sci USA* 91:12130–12134.
6. Gidwani A, Holowka D, Baird B (2001) *Biochemistry* 40:12422–12429.
7. Ge MT, Gidwani A, Brown HA, Holowka D, Baird B, Freed JH (2003) *Biophys J* 85:1278–1288.
8. London E (2002) *Curr Opin Struct Biol* 12:480–486.
9. Anderson RGW, Jacobson K (2002) *Science* 296:1821–1825.
10. Engelman DM (2005) *Nature* 438:578–580.
11. Ryan TA, Myers J, Holowka D, Baird B, Webb WW (1988) *Science* 239:61–64.
12. Hao MM, Mukherjee S, Maxfield FR (2001) *Proc Natl Acad Sci USA* 98:13072–13077.
13. Mayor S, Rao M (2004) *Traffic* 5:231–240.
14. Baumgart T, Hess ST, Webb WW (2003) *Nature* 425:821–824.
15. Holowka D, Baird B (1983) *Biochemistry* 22:3466.
16. Scott R, Maercklein P (1979) *J Cell Sci* 35:245–252.
17. Scott RE (1976) *Science* 194:743–745.
18. Wu ES, Tank DW, Webb WW (1982) *Proc Natl Acad Sci USA* 79:4962–4966.
19. Tank DW, Wu ES, Webb WW (1982) *J Cell Biol* 92:207–212.
20. Barak LS, Webb WW (1982) *J Cell Biol* 95:846–852.
21. Pyenta PS, Holowka D, Baird B (2001) *Biophys J* 80:2120–2132.
22. Korlach J, Schwille P, Webb WW, Feigenson GW (1999) *Proc Natl Acad Sci USA* 96:8461–8466.
23. Scott R, Perkins R, Zschunke M, Hoerl B, Maercklein P (1979) *J Cell Sci* 35:229–243.
24. Fridriksson EK, Shipkova PA, Sheets E, Holowka D, Baird BA, McLafferty FM (1999) *Biochemistry* 38:8056–8063.
25. Parton RG, Richards AA (2003) *Traffic* 2003:724–738.
26. Kahya N, Scherfeld D, Bacia K, Poolman B, Schwille P (2003) *J Biol Chem* 278:28109–28115.
27. Hammond AT, Heberle FA, Baumgart T, Holowka D, Baird B, Feigenson GW (2005) *Proc Natl Acad Sci USA* 102:6320–6325.
28. Thomas J, Holowka D, Baird B, Webb W (1994) *J Cell Biol* 125:795–802.
29. Pierini L, Holowka D, Baird B (1996) *J Cell Biol* 134:1427–1439.
30. Gerke V, Creutz CE, Moss SE (2005) *Nat Rev Mol Cell Biol* 6:449–461.
31. Sims PJ, Wiedmer T (2001) *Thromb Haemost* 86:266–275.
32. Ayuyan AG, Cohen FS (2006) *Biophys J* 91:2172–2183.
33. Yavin E, Zutra A (1979) *Biochim Biophys Acta* 553:424–437.
34. Brown DA, London E (2000) *J Biol Chem* 275:17221–17224.
35. Sheets ED, Holowka D, Baird B (1999) *J Cell Biol* 145:877–887.
36. Varma R, Mayor S (1998) *Nature* 394:798–801.
37. Friedrichson T, Kurzchalia TV (1998) *Nature* 394:802–805.
38. Dietrich C, Bagatolli LA, Volovyk ZN, Thompson NL, Levi M, Jacobson K, Gratton E (2001) *Biophys J* 80:1417–1428.
39. Kovarova M, Tolar P, Arudchandran R, Draberova L, Rivera J, Draber P (2001) *Mol Cell Biol* 21:8318–8328.
40. Larson DR, Gosse JA, Holowka DA, Baird BA, Webb WW (2005) *J Cell Biol* 171:527–536.
41. Field KA, Holowka D, Baird B (1995) *Proc Natl Acad Sci USA* 92:9201–9205.
42. Young RM, Holowka D, Baird B (2003) *J Biol Chem* 278:20746–20752.
43. Field K, Holowka D, Baird B (1997) *J Biol Chem* 272:4276–4280.
44. Field K, Holowka D, Baird B (1999) *J Biol Chem* 274:1753–1758.
45. Veatch SL, Keller SL (2003) *Biophys J* 85:3074–3083.
46. Staneva G, Angelova MI, Koumanov K (2004) *Chem Phys Lipids* 129:53–62.
47. Bacia K, Schwille P, Kurzchalia T (2005) *Proc Natl Acad Sci USA* 102:3272–3277.
48. Baumgart T, Das S, Webb WW, Jenkins JT (2005) *Biophys J* 89:1067–1080.
49. Seul M, Andelman D (1995) *Science* 267:476–483.
50. Samsonov AV, Mihalyov I, Cohen FS (2001) *Biophys J* 81:1486–1500.
51. Sharma P, Sabharanjak S, Mayor S (2002) *Cell Dev Biol* 13:205–214.
52. Keller H, Rentsch P, Hagmann J (2002) *Exp Cell Res* 277:161–172.
53. Trump BF, Berezesky IK (1998) in *When Cells Die: A Comprehensive Evaluation of Apoptosis and Programmed Cell Death*, eds Lockshin R, Zakeri Z, Tilly JL (Wiley–Liss, New York), pp 57–96.
54. Solsona C, Innocenti B, Fernandez JM (1998) *Biophys J* 74:1061–1073.
55. Swamy MJ, Ciani L, Ge MT, Smith AK, Holowka D, Baird B, Freed JH (2006) *Biophys J* 90:4452–4465.
56. Thomas JL, Feder TJ, Webb WW (1992) *Biophys J* 61:1402–1412.
57. Webb WW, Barak LS, Tank DW, Wu ES (1982) *Biochem Soc Symp* 46:191–205.
58. Hagelberg C, Allan D (1990) *Biochem J* 271:831–834.
59. Menon AK, Holowka D, Webb WW, Baird B (1986) *J Cell Biol* 102:541–550.
60. Menon A, Holowka D, Webb W, Baird B (1986) *J Cell Biol* 102:534–540.
61. Meder D, Moreno MJ, Verkade P, Vaz WLC, Simons K (2006) *Proc Natl Acad Sci USA* 103:329–334.
62. Kirkwood JG, Goldberg RJ (1950) *J Chem Phys* 18:54–57.
63. Stanley HE (1971) *Introduction to Phase Transitions and Critical Phenomena* (Clarendon, Oxford).
64. Simons K, Vaz WLC (2004) *Ann Rev Biophys Biomol Struct* 33:269–295.

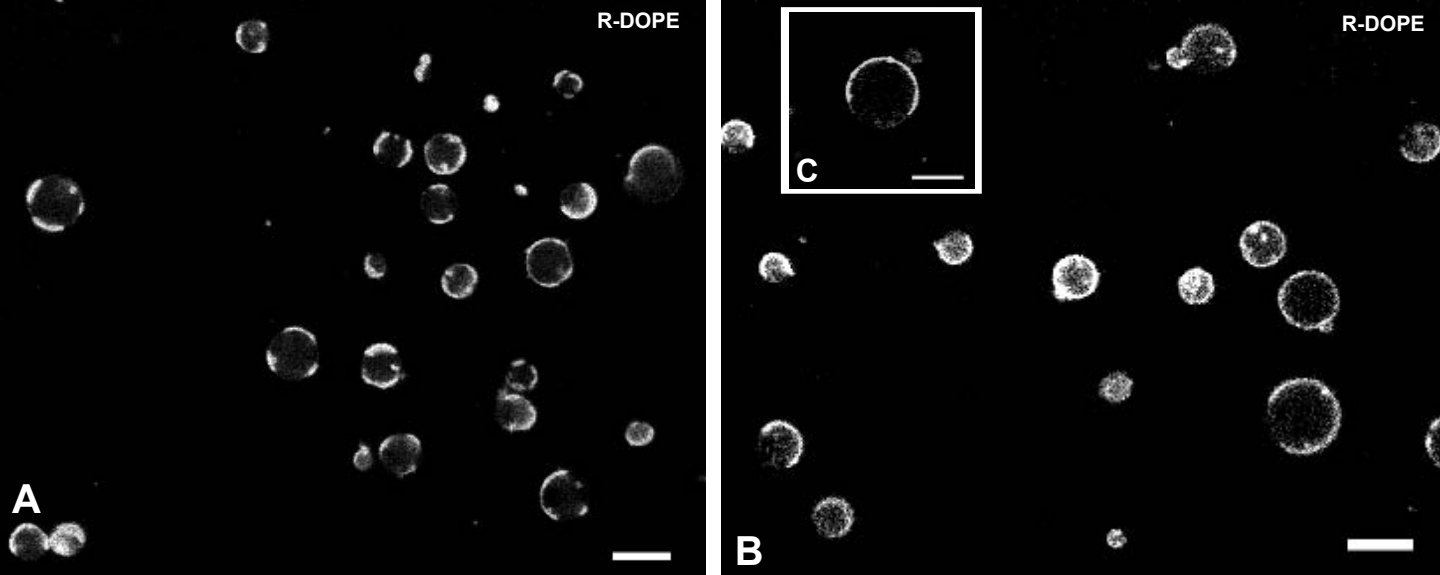
R-DOPE
A
R-DOPE
C
B

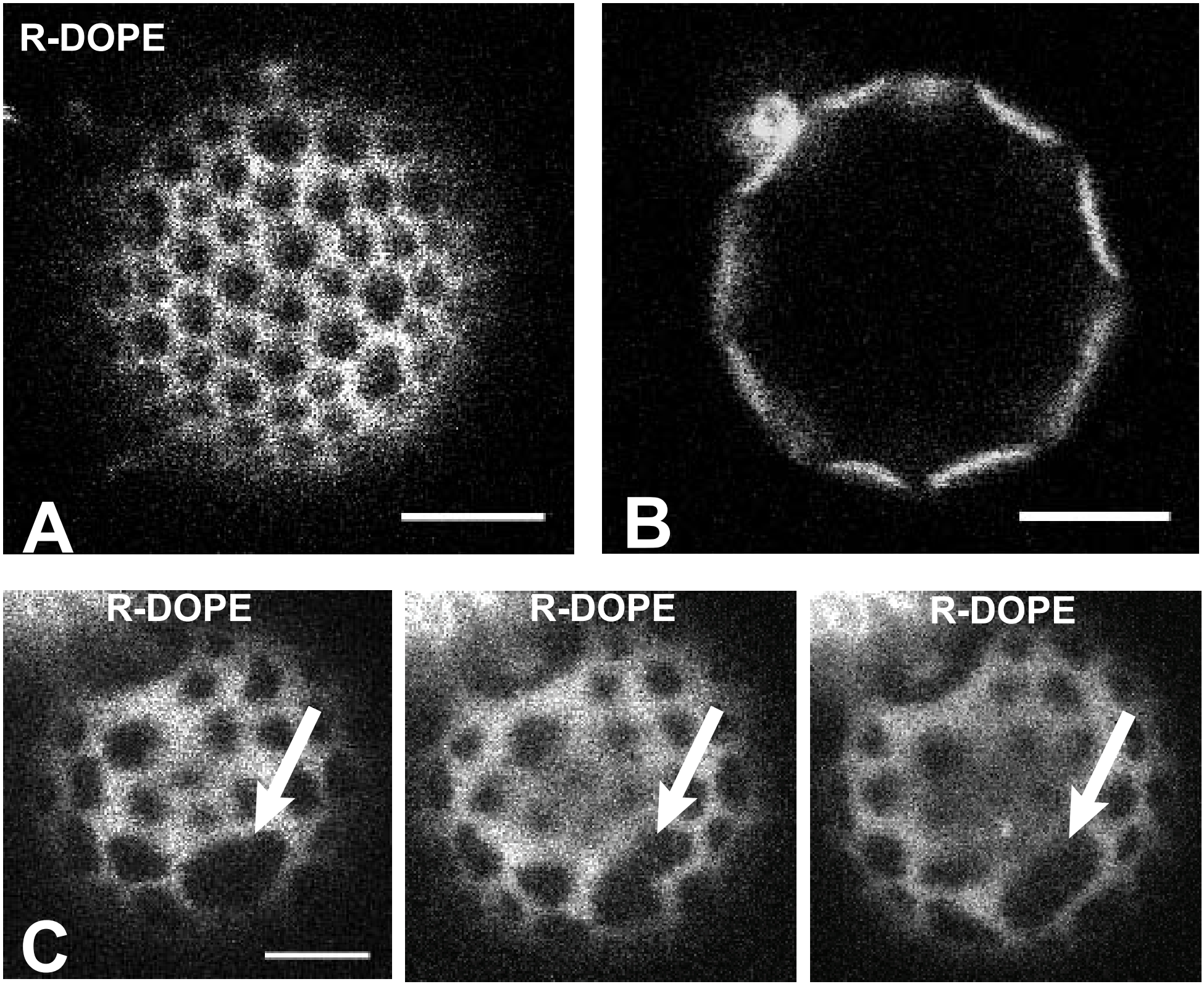
R-DOPE
A
B
R-DOPE
C
R-DOPE
R-DOPE